



Published in final edited form as:

J Phys Chem B. 2008 November 6; 112(44): 13765–13771. doi:10.1021/jp8062977.

Effects of Hofmeister Anions on the Phase Transition Temperature of Elastin-like Polypeptides

Younhee Cho[†], Yanjie Zhang[†], Trine Christensen[‡], Laura B. Sagle[†], Ashutosh Chilkoti[‡], and Paul S. Cremer^{*,†}

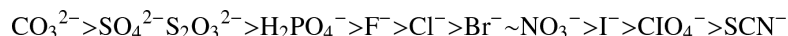
Department of Chemistry, Texas A&M University, College Station, Texas 77843, and Department of Biomedical Engineering, Duke University, Durham, North Carolina 27708

Abstract

The modulation of the lower critical solution temperature (LCST) of two elastin-like polypeptides (ELPs) was investigated in the presence of 11 sodium salts that span the Hofmeister series for anions. It was found that the hydrophobic collapse/aggregation of these ELPs generally followed the series. Specifically, kosmotropic anions decreased the LCST by polarizing interfacial water molecules involved in hydrating amide groups on the ELPs. On the other hand, chaotropic anions lowered the LCST through a surface tension effect. Additionally, chaotropic anions showed salting-in properties at low salt concentrations that were related to the saturation binding of anions with the biopolymers. These overall mechanistic effects were similar to those previously found for the hydrophobic collapse and aggregation of poly(*N*-isopropylacrylamide), PNIPAM. There is, however, a crucial difference between PNIPAM and ELPs. Namely, PNIPAM undergoes a two-step collapse process as a function of temperature in the presence of sufficient concentrations of kosmotropic salts. By contrast, ELPs undergo collapse in a single step in all cases studied herein. This suggests that the removal of water molecules from around the amide moieties triggers the removal of hydrophobic hydration waters in a highly coupled process. There are also some key differences between the LCST behavior of the two ELPs. Specifically, the more hydrophilic ELP V₅A₂G₃-120 construct displays collapse/aggregation behavior that is consistent with a higher concentration of anions partitioning to polymer/aqueous interface as compared to the more hydrophobic ELP V₅-120. It was also found that larger anions could bind with ELP V₅A₂G₃-120 more readily in comparison with ELP V₅-120. These latter results were interpreted in terms of relative binding site accessibility of the anion for the ELP.

Introduction

Inorganic salts have a strong effect on protein solubility. For this reason, salt-induced protein precipitation is frequently used in protein purification processes.¹ The solubility of proteins in different salt solutions typically follows a recurring trend, known as the Hofmeister series.^{2–4} The effects associated with this trend are typically more pronounced for anions than cations. The anion series is as follows:



© 2008 American Chemical Society

*Corresponding author: cremer@mail.chem.tamu.edu.

[†]Texas A&M University.

[‡]Duke University.

Supporting Information Available: Raw data for light scattering as a function of position across individual capillary tubes and the corresponding determination of the LCST. This material is available free of charge via the Internet at <http://pubs.acs.org>.

The anions can be categorized into two general groups based upon the physical behavior of aqueous–macromolecular systems in their presence. Specifically, species to the left of Cl^- are called kosmotropes and have been shown to salt protein molecules out of solution. On the other hand, species to the right of Cl^- are called chaotropes and are known to increase the solubility of protein molecules in solution.⁵

Since it was first discovered 120 years ago, the Hofmeister series has been found to apply to a plethora of biological and chemical phenomena in addition to protein precipitation. These include protein crystallization, enzyme turnover rates, and micelle formation.^{6–10} Despite its wide use, a molecular level understanding of this series has remained elusive for over a century.^{11–14} Recently, it has been shown that the ability of a particular salt to affect the structure of water in bulk solution probably plays little, if any, role in the Hofmeister effect.^{11–16} For example, Bakker and co-workers reported that the presence of SO_4^{2-} or ClO_4^- ions does not affect the hydrogen-bonding network of water beyond the first hydration shell.^{13,14} Pielak and co-workers demonstrated that the solute's impact on water structure is not correlated to its effect on protein stability.¹¹ Furthermore, our laboratory has shown that water molecules adjacent to a Langmuir monolayer do not necessarily show structural variations consistent with this series even when the physical properties of the monolayer itself strictly follow the series.¹² Most recently, Saykally and Geissler have investigated the Raman spectra of aqueous salt solutions. Their work also shows little evidence of bulk water structure making and breaking effects for the ions.¹⁵

In contrast to the role of ions on water structure, it has been demonstrated that direct interactions between ions and macromolecules can be key to understanding the Hofmeister series.^{17–21} In fact, proposed mechanisms to explain the physical properties of macromolecules in solution have involved dispersion forces, ion binding to the macromolecules, and the modulation of surface tension by the ions.^{17–19,21–26} Recently, our laboratory has reported the effects of Hofmeister anions on the lower critical solution temperature (LCST) of poly(*N*-isopropylacrylamide), PNIPAM. This work, which studied the effects of 11 different anions, showed that changes in the LCST of PNIPAM were caused by completely different mechanisms for chaotropes and kosmotropes.²⁷ Specifically, chaotropic anions lowered the LCST by increasing the surface tension at the polymer/water interface at higher salt concentrations. At lower salt concentrations, the anions raised the LCST through a direct binding mechanism that followed a Langmuir isotherm. On the other hand, kosmotropic anions generally decreased the LCST of the polymer by polarizing interfacial water molecules. This polarization effect weakened the hydrogen bonding of water molecules to the lone pairs on the oxygen of the amide groups in PNIPAM.

PNIPAM consists of monomers that are isomers of isoleucine, and its LCST is thought to be a good mimic for the cold denaturation of proteins.²⁸ The key difference between this polymer and a polypeptide is that the amide moiety is pendent rather than part of the backbone (Figure 1). Therefore, it is important to determine whether the mechanism that governs the modulation of the LCST of PNIPAM as salts are added to solution can be extended to the much more important case of polypeptides. To this end, we have employed elastin-like polypeptides (ELPs) as a model polypeptide system, which also exhibits LCST phase behavior.

We chose ELPs as a model for more complex protein constructs. Like proteins, ELPs are composed of amino acids so that the sequence and chain length of ELPs can be precisely controlled by recombinant synthesis.^{29,30} Unlike proteins, however, which typically have nonrepetitive sequences and well-defined tertiary structures, ELPs are considerably simpler repetitive polypeptides that consist of a five-residue repeat, VPGXG, whereby X can be any amino acid except proline. Therefore, ELPs are a simple but powerful model to carry out

systematic structure–property studies of polypeptides in solution. Significant sequence diversity can be achieved by substituting various amino acids at the fourth position.

Like PNIPAM, ELPs precipitate from solutions above their LCST value.^{31–37} However, PNIPAM undergoes hydrophobic collapse/aggregation without the formation of specific secondary or tertiary structures. On the other hand, the collapse and aggregation of ELPs is associated with significant β -turn/ β -spiral secondary/tertiary structure formation.^{38–44} Such properties afford an interesting bridge between the purely LCST-driven behavior of PNIPAM and the more complex folding and cold denaturation behavior exhibited by typical proteins.

Herein, Hofmeister effects were investigated for two different ELPs using 11 different sodium salts. The ELPs employed were ELP V₅-120 and ELP V₅A₂G₃-120. Both molecules consist of 120 repeats of the VPGXG sequence. However, the first molecule has V at all guest residue positions, while the second, more hydrophilic ELP contains a mixture of V, A, and G guest residues in a 5:2:3 ratio. The results of the present ELP studies showed a general correlation with data from PNIPAM,²⁷ although several key differences were also found.

The overall mechanism for the modulation of the LCST is presented in Figure 2. As shown, the kosmotropic anions weaken the hydrogen bonding of water to the carbonyl moiety of the amide backbone (Figure 2a). This effect is manifest by a strong correlation between the change in the LCST of the ELP and the entropy of hydration values for the kosmotropes. By contrast, chaotropes depress the LCST values by weakening the hydrophobic hydration of the biomacromolecule (Figure 2b). Evidence for this effect comes from a strong correlation between the LCST of the biopolymers and the surface tension increment values, σ , for the anions. Concomitantly with salting-out effects, there is also a salting-in effect caused by direct binding of chaotropic anions with the amide moieties (Figure 2c). This direct ion binding effect shows Langmuir isotherm type behavior. It should be noted that the effects described in Figure 2a,b were found to be correlated with a linear decrease in the LCST of the ELPs per mole of added salt, while the effect shown in Figure 2c was associated with an increase in the LCST and was a saturation effect.

Experimental Section

ELP Preparation

The pET plasmids employed herein were constructed using recursive directional ligation as previously described.²⁹ The plasmids were expressed in BLR/DE3 *E. coli* in high growth media (TBdry) supplemented with ampicillin. Expression was carried out for 24 h without isopropyl- β -D-thiogalactoside induction and resulted in typical yields of 200–300 mg per liter of cell culture medium. Purification of the ELP was done via sonication of the cells followed by a series of inverse transition cycling (ITC) steps. For example, one round of ITC was carried out by centrifugation at 10000*g* at 50 °C by adding 1 M NaCl. The pellets (containing ELP) were then dissolved in phosphate buffer (10 mM, pH 6.9, 4 °C), and the remaining cellular debris was removed by centrifugation at 10000*g*. Typically, two rounds of ITC were needed to remove impurities. The molecular weight and purity of the ELPs were assessed by SDS-PAGE and CuCl₂ staining. The concentrations of the purified ELP solutions were determined by measuring the absorbance at 280 nm ($\epsilon = 5690 \text{ M}^{-1} \text{ cm}^{-1}$). After purification by ITC, samples were dialyzed against purified water (NANOpure Ultrapure Water System, Barnstead, Dubuque, IA) with a minimum resistivity of 18 M Ω · cm to remove residual salts. Finally, the samples were lyophilized and stored at –80 °C until use.

LCST Measurements

NaSCN, NaI, NaClO₄, NaBr, NaNO₃, NaCl, NaF, NaH₂PO₄, Na₂S₂O₃, Na₂SO₄, and Na₂CO₃ were purchased from Sigma Aldrich (>99% purity). The salts were dissolved in 10 mM phosphate buffer (pH 6.9) made with purified water from the NANOpure Ultrapure Water System. ELPs were dissolved in salt solutions at a polypeptide concentration of 6.4 mg/mL. The LCST values of the ELP solutions were measured using a microfluidic temperature-gradient apparatus placed under a dark field microscope.⁴⁵ The temperature-gradient apparatus consisted of two brass tubes ($\frac{1}{8}$ in. wide, K&S Engineering, Chicago, IL) placed parallel to each other. A hot solution was flowed inside one tube while a cold solution was flowed inside the other to create a linear temperature gradient over a 5 mm gap between them.^{46–48} A cover glass was placed over the brass tubes as a sample stage. ELP solutions were placed inside rectangular borosilicate capillary tubes (VitroCom, Inc.) with dimensions of 2 cm \times 1 mm \times 100 μ m (length \times width \times height). Six tubes were placed on the sample stage with their long axis parallel to the temperature gradient. In each case, four capillaries contained samples while the other two tubes contained standards with known LCST values to calibrate the temperature gradient. The standard solutions were 10 mg/mL PNIPAM in water without salt and 10 mg/mL PNIPAM in 0.35 M KCl, which had LCST values of 30.9 and 26.5 $^{\circ}$ C, respectively. For high-temperature measurements (above 40 $^{\circ}$ C) two organic standards, octadecanol and 1,2-decanethiol, were used. The melting temperatures of the organic samples were determined independently in a melting temperature apparatus (Optimelt MPA100, Stanford Research System) and had values of 58.5 ± 0.3 for octadecanol and 46.1 ± 0.2 for 1,2-decanethiol.

In a typical experiment, six capillary tubes were placed side-by-side and imaged by dark field microscopy with a 2 \times objective under an inverted microscope (TE2000-U, Nikon). Light scattering images from the capillary tubes were captured with a CCD camera (Micromax 1024, Princeton Instruments) using dark field optics. The LCST of the ELPs and PNIPAM were measured as an abrupt change in the amount of light scattering found in a dark field image.^{27,45,49} The reversibility of the LCST process was verified by gently sliding the capillary tubes back and forth along the temperature gradient. This procedure confirmed that the LCST always occurred at the identical position along the gradient after equilibrium had been achieved. It should be noted that there is a sharp increase in the amount of light scattered at temperatures above which the polypeptides undergo hydrophobic collapse/aggregation. On the other hand, the organic samples scattered significantly more light in the solid state than above their melting point. The temperature along the long axis of the tube was assumed to vary linearly as a function of distance as has been previously shown.^{46–48} Metamorph software (Universal Imaging Corp.) was used to create line profiles of light scattering as a function of position. These line profiles were used to abstract the exact phase transition temperatures following our standard procedures. All LCST values reported herein represent an average of eight measurements.

Results

LCST of ELP V₅-120 with Hofmeister Salts

In a first set of experiments, the LCST values of ELP V₅-120 were determined as a function of salt type and concentration for the 11 sodium salts investigated (Figure 3). The phase transition occurs at \sim 28 $^{\circ}$ C in the absence of salt. Moreover, the kosmotropic anions F⁻, H₂PO₄⁻, S₂O₃²⁻, SO₄²⁻, CO₃²⁻, and Cl⁻ display linear salting-out behavior. The data from these anions can be fit by a simple linear equation:

$$T = T_0 + c[M] \quad (1)$$

whereby T_0 is the LCST value in the absence of salt. The term c is a constant with units of temperature/molarity, and $[M]$ is the molar concentration of salt. The c values for these kosmotropes are reported in Table 1.

In contrast with the kosmotropes, the chaotropic anions (SCN^- , I^- , ClO_4^- , Br^- , NO_3^-) show nonlinear changes in their LCST values as a function of added salt. In fact, the LCST values for SCN^- and I^- actually increase at low salt concentration before salting-out behavior becomes dominant at higher salt concentration. The shape of these curves can be well fit by adding a binding isotherm to the linear term used for the kosmotropes (eq 2):

$$T = T_0 + c[M] + \frac{B_{\max} K_A [M]}{1 + K_A [M]} \quad (2)$$

The first two terms in eq 2 have the same meanings as in eq 1. The last term is a Langmuir binding isotherm, where K_A is the apparent equilibrium association constant. Since the isotherm is unitless, a constant, B_{\max} , is added, which has units of temperature. This constant is interpreted as the increase in the LCST value found when a saturation concentration of salt is present. The B_{\max} , K_A , and c values determined with the chaotropic anions are reported in Table 1.

The c values for ELP V₅-120 in the presence of the 11 sodium salts are plotted against the known entropy of hydration values, ΔS_{hydr} ,⁵⁰ for each of the anions employed (Figure 4a). As can be seen, the correlation between c and ΔS_{hydr} is excellent for the kosmotropes, but not for the chaotropes. Changing the x -axis to the surface tension increment, σ , for each of the anions shows excellent correlation to the chaotropes, but the kosmotropes are uncorrelated (Figure 4b). It should be noted that the surface tension increment refers to the measured change in surface tension at the air/water interface per mole of salt added to the solution. It should be further noted that the c values were also tested against other thermodynamic parameters such as polarizability, ionic volume, viscosity coefficient, enthalpy of hydration, and free energy of hydration; however, the data were uncorrelated. Significantly, the trends found here were identical to the ones previously found for the LCST of PNIPAM.²⁷ Namely, the entropies of hydration were correlated with the c values of the kosmotropes, while the surface tension increments were correlated with the c values of the chaotropes.

In addition to the linear portion of the LCST vs salt concentration curves shown in Figure 3, there is also a nonlinear portion for the chaotropic anions. This can be directly visualized by subtracting out the linear contribution to the curves in Figure 3 and replotting the data (Figure 5). The binding curves are clearly revealed by this procedure. Significantly, they show a reasonably good fit to a Langmuir isotherm (dashed lines).

LCST of ELP V₅A₂G₃-120 with Hofmeister Salts

A slightly less hydrophobic biomacromolecule, ELP V₅A₂G₃-120, was chosen for a second set of experiments in order to ascertain the dependence of the LCST behavior on the amino acid sequence of the ELP. The polymer chain length of ELP V₅A₂G₃-120 was the same as ELP V₅-120, but half of the valine residues were replaced with glycines and alanines. Again, temperature-dependent aggregation behavior was measured in the presence of the same 11 Hofmeister salts to directly compare the LCST values with ELP V₅-120 (Figure 6). As can be seen, the general trends are similar to those seen for ELP V₅-120. The data were again fit with eqs 1 and 2, and the associated values of c , K_A , and B_{\max} are provided in Table 1. Furthermore, the correlation between the c values of the kosmotropes and ΔS_{hydr} was excellent (Figure 7a). The correlation between σ and the c values for the chaotropes was also

quite good (Figure 7b). Finally, the residual portion of the LCST vs salt concentration curves are plotted for the chaotropic ions in Figure 8 after the linear portions were subtracted out. Again, the data show evidence for a saturation binding phenomenon. The dashed lines in this figure are the apparent fits to the Langmuir isotherm equation.

Discussion

Mechanisms for Modulating the LCST of ELPs by Salts

The data shown in Figures 3–8 are consistent with the mechanism for modulating the LCST of ELPs by Hofmeister anions presented in Figure 2. Specifically, kosmotropic ions modulate the phase transition temperature through the polarization of water molecules in the first hydration shell of the biopolymer (Figure 2a). Evidence for this statement comes from Figures 4a and 7a, which show that changes in the LCST are directly correlated to the entropies of hydration of the kosmotropes, but not for the chaotropes. Indeed, kosmotropic anions are well hydrated and are able to strongly attract protons of water molecules in their first hydration shell. This, in turn, leaves the rest of the water molecule more negatively charged. If the same water molecule is also hydrogen bonded to the amide group of the ELP, then the bond should be weakened by the polarization effect. This ability of kosmotropes to polarize water molecules is manifest at the macroscopic level by their ability to order water molecules around themselves and thereby lower the entropy of the aqueous solution, ΔS_{hydr} .⁵¹ By contrast, the chaotropes cannot sufficiently polarize polymer-associated water molecules to weaken the hydration of the amide moieties. Instead, the depression of the LCST comes from the destabilization of hydrophobic hydration waters. Evidence for this statement can be found in Figures 4b and 7b. As can be seen, there is a linear correlation between the surface tension increment of the chaotropic anions and the corresponding c value.

As noted above, the water polarization effect for kosmotropes and the surface tension increment effect for chaotropes are expected to cause the LCST of the ELPs to decrease linearly with salt concentration. This should be the case for the chaotropes because the surface tension of aqueous interfaces varies linearly with salt concentration.^{25,52} Furthermore, one might also expect the polarization effect to be linearly dependent on the concentration of salt because no specific binding sites are involved.^{18,25,53} On the other hand, the nonlinear component of the salting-in effect for the chaotropes follows saturation binding behavior (Figures 5 and 8). This is consistent with the notion that the amide dipoles serve as putative binding sites for these anions. Such binding interactions will increase the charge on the biomacromolecule and thereby inhibit hydrophobic collapse. It should be noted that the K_A values found for this system should be treated as only apparent association constants. Indeed, the measured LCST values for a given salt can vary by almost 30 °C as the salt concentration is increased with ELP V₅A₂G₃-120 (Figure 6). Therefore, the experiments are not conducted isothermally. Moreover, binding should be anticooperative because it should become increasingly difficult to bind larger numbers of anions to the same polymer chain.⁵⁴ This should be the case because the binding of one anion repels the binding of additional anions by electrostatics. Nevertheless, the residual curves abstracted in Figures 5 and 8 are in reasonably good agreement with previous measurements of anion binding to amide moieties.¹⁷ Specifically, the K_A values are in the same range as previous results. Also, the finding that more chaotropic anions bind more tightly than less chaotropic anions is in agreement with previous results.

Finally, Cl⁻ represents a somewhat anomalous case. Although the change in the LCST as a function of the NaCl concentration was linear like the kosmotropes (Figures 3 and 6), the thermodynamic correlation for Cl⁻ was to σ , like the chaotropes (Figures 4b and 7b). In other words, this ion's ΔS_{hydr} is sufficiently small that it does not cause induced polarization

effects. However, the ion is sufficiently well hydrated that it does not noticeably bind to the polypeptide chains like the chaotropes. Thus, this ion represents intermediate behavior.

Comparison with PNIPAM

As noted above, our laboratory has previously measured the effects of Hofmeister salts on the LCST of PNIPAM.²⁷ The data for ELPs fit to the same sets of equations as PNIPAM with the same correlations among c values, ΔS_{hydr} , and σ . Moreover, a Langmuir isotherm fits the nonlinear portions of the chaotropic data. Such remarkable similarities speak to the general nature of our proposed mechanism for the modulation of hydrophobic collapse of uncharged polymers by salts.

In addition to similarities, there are also some significant differences between the behavior of ELPs and PNIPAM in the presence of salts. Most importantly, PNIPAM undergoes a two-step collapse process in the presence of sufficient concentrations of kosmotropic ions.^{27,45} For example, in the presence of 200 mM Na_2SO_4 , a 10 mg/mL solution of PNIPAM undergoes partial collapse near 24 °C and full collapse above 26 °C. The partial collapse to a molten globule state manifests itself as a level of light scattering from the polymer solution which is intermediate between the high level found upon full hydrophobic collapse and the relatively low level that exists when the polymer solution is below the LCST. In contrast with the PNIPAM data, no evidence was found in the present study for a thermodynamically stable molten globule state for the ELPs.

The partial collapse of PNIPAM was interpreted to arise from the separate dehydration of the amide moieties and the hydrophobic portions of the macromolecule. Evidently, the hydration waters could be removed from the amide moieties while the hydrophobic hydration waters remained intact. Corroborating evidence for this hypothesis came from subsequently performed NMR studies.⁵⁵ The key difference between the chemical structures of PNIPAM and the ELPs is the fact that the amide groups are pendent in acrylamide polymers, but part of the backbone in polypeptides. Apparently, when the amide groups are part of the backbone, removal of their hydration waters necessarily triggers the removal of hydrophobic hydration waters as well. On the other hand, when amide groups are pendent, the two processes can be decoupled.

ELP V₅-120 vs ELP V₅A₂G₃-120

Both biopolymers investigated in the present study showed similar qualitative phase transition behavior as the specific ion identity and concentration were modulated. Nevertheless, there appears to be some key differences in the behavior of the two systems. For example, the LCST value, T_0 , of ELP V₅A₂G₃-120 without added salt is about 14 °C higher than that of ELP V₅-120. This is due to the presence of less hydrophobic residues such as alanine and glycine. Moreover, the c values were generally greater for V₅A₂G₃-120 than for the more hydrophobic V₅-120 biopolymer. This trend was found with both the kosmotropes and chaotropes. Such a universal trend almost certainly reflects a more favorable partitioning of ions from bulk solution to the aqueous/polymer interface with the less hydrophobic polymer.⁵⁶

More chemically specific information about the two polymers can be inferred by examining differences in B_{max} values for the chaotropic anions. Specifically, the higher values of B_{max} for ELP V₅A₂G₃-120 should be correlated with a larger number of bound anions.⁴⁵ This is consistent with the more open structure of the polymer. However, the magnitude of the difference between the two polymers should be ion specific and depend upon the ionic volume for a given chaotropic anion. For sufficiently small anions, the effect should be rather limited as they would be able to equally access binding sites on both polymers. On the

other hand, bigger ions should be more strongly inhibited from binding to at least some sites on ELP V₅-120 in comparison with the more open ELP V₅A₂G₃-120 construct.

To help quantify ion specific differences in binding site accessibility, the ratios of B_{\max} values for the two polymers are provided in Table 1 [$B_{\max}(\text{V}_5\text{A}_2\text{G}_3)/B_{\max}(\text{V}_5)$]. A plot of this ratio against the ionic volume of each of the chaotropic anions is provided in Figure 9. As can be seen, a linear trend between the B_{\max} ratio and ionic volume is observed. As expected, the largest anion, ClO_4^- , has the largest ratio, while the effect of Br^- is more modest. Moreover, it appears that there is a cutoff for this effect around an ionic volume of 25 cm^3/mol . In other words, binding for anions with volumes below this particular size would be expected to have a B_{\max} ratio of 1.0.

Probing Other Systems

The data from ELP V₅-120 and V₅A₂G₃-120 clearly show that ELPs can be employed to glean information about specific ion effects on hydrophobic collapse. The fact that the fourth residue in the pentameric repeat is a guest residue holds out the very promising prospect for investigating the influence of specific residues on Hofmeister behavior. For example, the addition of charged residues such as D, E, R, and K should allow screening effects for both cationic and anionic polymers to be considered. On the other hand, the use of F residues would be advantageous for the investigation of cation- π interactions. Exactly these types of investigation are presently underway in our laboratories.

Supplementary Material

Refer to Web version on PubMed Central for supplementary material.

Acknowledgments

We thank the National Institutes of Health (R01 GM070622 to P.C. and R01 GM61232 to A.C.) as well as the Robert A. Welch Foundation (grant A-1421 to P.C.) for support.

References and Notes

1. Baldwin RL. *Biophys J.* 1996; 71:2056. [PubMed: 8889180]
2. Hofmeister F. *Arch Exp Pathol Pharmacol.* 1888; 24:247.
3. Collins KD, Washabaugh MW. *Q Rev Biophys.* 1985; 18:323. [PubMed: 3916340]
4. Kunz W, Henle J, Ninham BW. *Curr Opin Colloid Interface Sci.* 2004; 9:19.
5. Kunz W, Lo Nostro P, Ninham BW. *Curr Opin Colloid Interface Sci.* 2004; 9:1.
6. Bostrom M, Williams DRM, Ninham BW. *Langmuir.* 2002; 18:6010.
7. Craig VSJ. *Curr Opin Colloid Interface Sci.* 2004; 9:178.
8. Salis A, Pinna MC, Bilanicova D, Monduzzi M, Lo Nostro P, Ninham BW. *J Phys Chem B.* 2006; 110:2949. [PubMed: 16471906]
9. Dexter AF. *J Phys Chem B.* 2005; 109:14750. [PubMed: 16852861]
10. Evans DF, Mitchell DJ, Ninham BW. *J Phys Chem.* 1984; 88:6344.
11. Batchelor JD, Olteanu A, Tripathy A, Pielak GJ. *J Am Chem Soc.* 2004; 126:1958. [PubMed: 14971928]
12. Gurau MC, Lim SM, Castellana ET, Albertorio F, Kataoka S, Cremer PS. *J Am Chem Soc.* 2004; 126:10522. [PubMed: 15327293]
13. Omta AW, Kropman MF, Woutersen S, Bakker HJ. *Science.* 2003; 301:347. [PubMed: 12869755]
14. Omta AW, Kropman MF, Woutersen S, Bakker HJ. *J Chem Phys.* 2003; 119:12457.
15. Smith JD, Saykally RJ, Geissler PL. *J Am Chem Soc.* 2007; 129:13847. [PubMed: 17958418]
16. Collins KD, Neilson GW, Enderby JE. *Biophys Chem.* 2007; 128:95. [PubMed: 17418479]

17. VonHippel PH, Peticola V, Schack L, Karlson L. *Biochemistry*. 1973; 12:1256. [PubMed: 4696753]
18. VonHippel PH, Schleich T. *Acc Chem Res*. 1969; 2:257.
19. VonHippel PH, Wong KY. *Science*. 1964; 145:577. [PubMed: 14163781]
20. Ninham BW, Yaminsky V. *Langmuir*. 1997; 13:2097.
21. Song JD, Ryoo R, Jhon MS. *Macromolecules*. 1991; 24:1727.
22. Bostrom M, Williams DRM, Ninham BW. *Phys Rev Lett*. 2001; 87:168103. [PubMed: 11690249]
23. Nandi PK, Robinson DR. *J Am Chem Soc*. 1972; 94:1299. [PubMed: 5060273]
24. Schellman JA. *Biophys J*. 2003; 85:108. [PubMed: 12829469]
25. Pegram LM, Record MT. *Proc Natl Acad Sci USA*. 2006; 103:14278. [PubMed: 16980410]
26. Pegram LM, Record MT. *J Phys Chem B*. 2007; 111:5411. [PubMed: 17432897]
27. Zhang YJ, Furyk S, Bergbreiter DE, Cremer PS. *J Am Chem Soc*. 2005; 127:14505. [PubMed: 16218647]
28. Tiktopulo EIUVN, Lushchik VB, Klenin SI, Bychkova VE, Ptitsyn OB. *Macromolecules*. 1995; 28:7519.
29. Meyer DE, Chilkoti A. *Biomacromolecules*. 2002; 3:357. [PubMed: 11888323]
30. Meyer DE, Chilkoti A. *Biomacromolecules*. 2004; 5:846. [PubMed: 15132671]
31. Meyer DE, Trabbic-Carlson K, Chilkoti A. *Biotechnol Prog*. 2001; 17:720. [PubMed: 11485434]
32. Nath N, Chilkoti A. *J Am Chem Soc*. 2001; 123:8197. [PubMed: 11516269]
33. Yamaoka T, Tamura T, Seto Y, Tada T, Kunugi S, Tirrell DA. *Biomacromolecules*. 2003; 4:1680. [PubMed: 14606895]
34. Trabbic-Carlson K, Meyer DE, Liu L, Piervincenzi R, Nath N, LaBean T, Chilkoti A. *Protein Eng, Des Sel*. 2004; 17:57. [PubMed: 14985538]
35. Urry DW, Luan CH, Parker TM, Gowda DC, Prasad KU, Reid MC, Safavy A. *J Am Chem Soc*. 1991; 113:4346.
36. Meyer DE, Chilkoti A. *Nat Biotechnol*. 1999; 17:1112. [PubMed: 10545920]
37. Reguera J, Urry DW, Parker TM, McPherson DT, Rodriguez-Cabello JC. *Biomacromolecules*. 2007; 8:354. [PubMed: 17291058]
38. Flamia R, Zhdan PA, Martino M, Castle JE, Tamburro AM. *Biomacromolecules*. 2004; 5:1511. [PubMed: 15244472]
39. Ohgo K, Ashida J, Kumashiro KK, Asakura T. *Macromolecules*. 2005; 38:6038.
40. Kumashiro KK, Kurano TL, Niemczura WP, Martino M, Tamburro AM. *Biopolymers*. 2003; 70:221. [PubMed: 14517910]
41. Ohgo K, Kurano TL, Kumashiro KK, Asakura T. *Biomacromolecules*. 2004; 5:744. [PubMed: 15132656]
42. Yao XL, Hong M. *J Am Chem Soc*. 2004; 126:4199. [PubMed: 15053609]
43. Schmidt P, Dybal J, Rodriguez-Cabello JC, Reboto V. *Biomacromolecules*. 2005; 6:697. [PubMed: 15762632]
44. Li B, Alonso DOV, Bennion BJ, Daggett V. *J Am Chem Soc*. 2001; 123:11991. [PubMed: 11724607]
45. Zhang Y, Furyk S, Sagle LB, Cho Y, Bergbreiter DE, Cremer PS. *J Phys Chem C*. 2007; 111:8916.
46. Mao HB, Holden MA, You M, Cremer PS. *Anal Chem*. 2002; 74:5071. [PubMed: 12380832]
47. Mao HB, Li CM, Zhang YJ, Bergbreiter DE, Cremer PS. *J Am Chem Soc*. 2003; 125:2850. [PubMed: 12617632]
48. Mao HB, Yang TL, Cremer PS. *J Am Chem Soc*. 2002; 124:4432. [PubMed: 11960472]
49. Zhang YJ, Mao HB, Cremer PS. *J Am Chem Soc*. 2003; 125:15630. [PubMed: 14664611]
50. Marcus, Y. *Ion Properties*. Marcel Dekker; New York: 1997.
51. Zangi R, Hagen M, Berne BJ. *J Am Chem Soc*. 2007; 129:4678. [PubMed: 17378564]
52. Jarvis NL, Scheiman MA. *J Phys Chem*. 1968; 72:74.
53. Jungwirth P, Tobias DJ. *Chem Rev*. 2006; 106:1259. [PubMed: 16608180]
54. Chen X, Yang T, Kataoka S, Cremer PS. *J Am Chem Soc*. 2007; 129:12272. [PubMed: 17880076]

55. Rice CV. *Biomacromolecules*. 2006; 7:2923. [PubMed: 17025371]
56. Leunissen ME, van Blaaderen A, Hollingsworth AD, Sullivan MT, Chaikin PM. *Proc Natl Acad Sci USA*. 2007; 104:2585. [PubMed: 17307876]

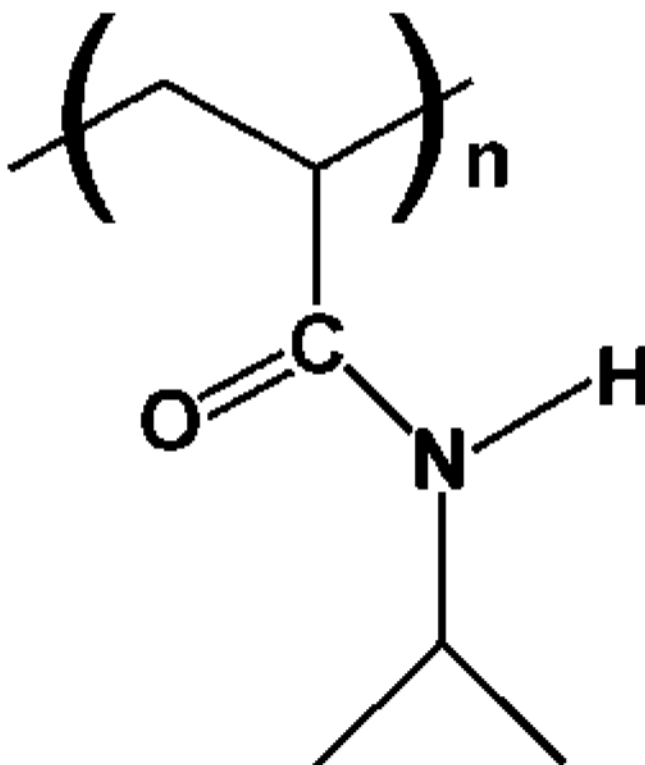


Figure 1.
Structure of PNIPAM.

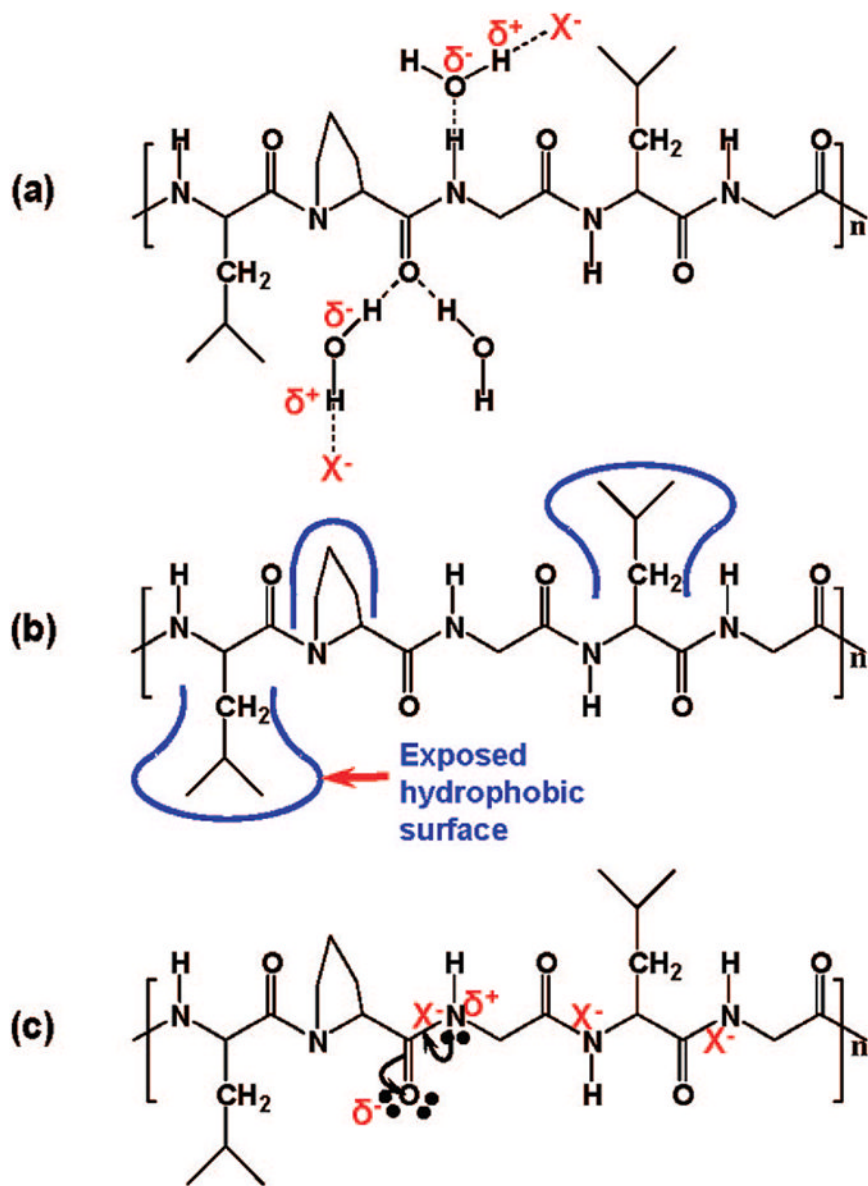


Figure 2. Proposed mechanisms for specific anion effects on the LCST of ELP V₅₋₁₂₀. (a) Direct interactions of anions with water involved in hydrogen bonding to the amide. Kosmotropic anions polarize these water molecules and thereby weaken the hydrogen bonding of water to the macromolecule, a salting-out effect. (b) The blue lines represent the hydrophobically hydrated regions of the biomacromolecule. The cost of such hydration increases as salt is added to solution. (c) Direct ion binding of chaotropic anions to the amide moieties along the backbone of the polypeptide should cause a salting-in effect.

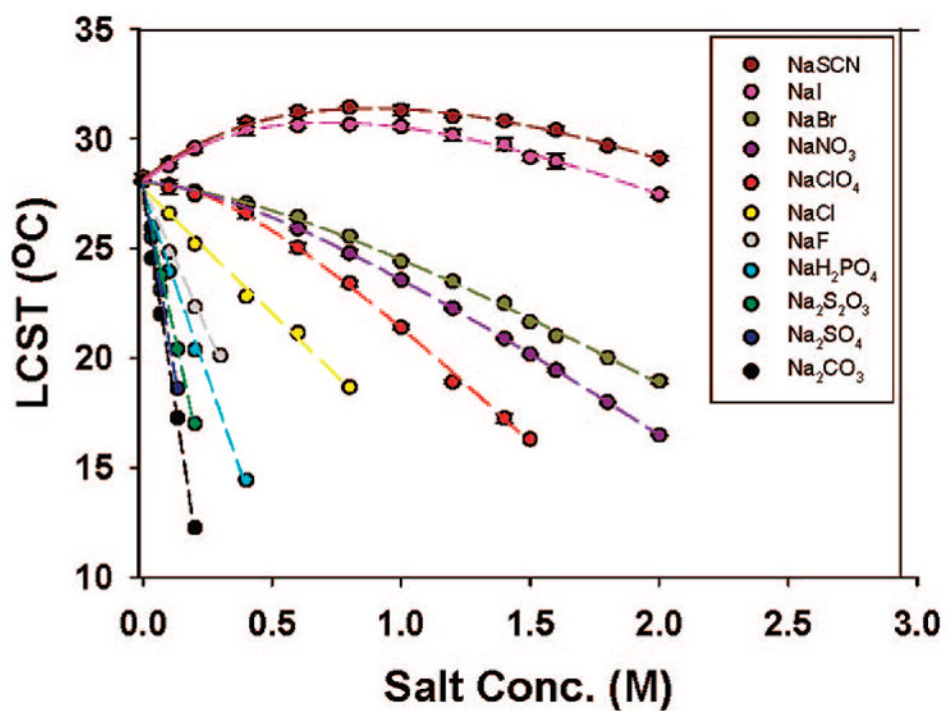


Figure 3. LCST vs salt concentration curves for a series of sodium salts with ELP V₅-120. Each data point represents the average of eight measurements, and the standard deviations are within the size of the circular data points in all cases. The dashed lines are fits to the data using eqs 1 and 2.

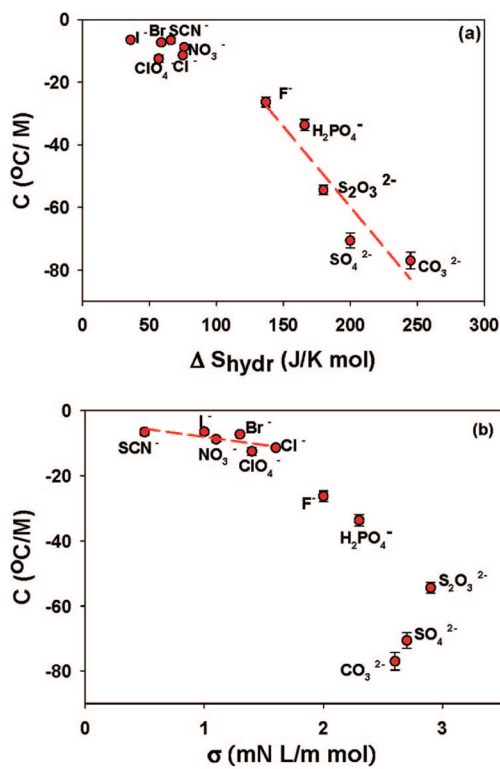


Figure 4. Plot of the linear slope, c , from eq 2 against (a) ΔS_{hydr} and (b) σ for ELP V₅-120 with 11 different sodium salts. The dashed red lines are fits to the kosmotropes in (a) and the chaotropes in (b).

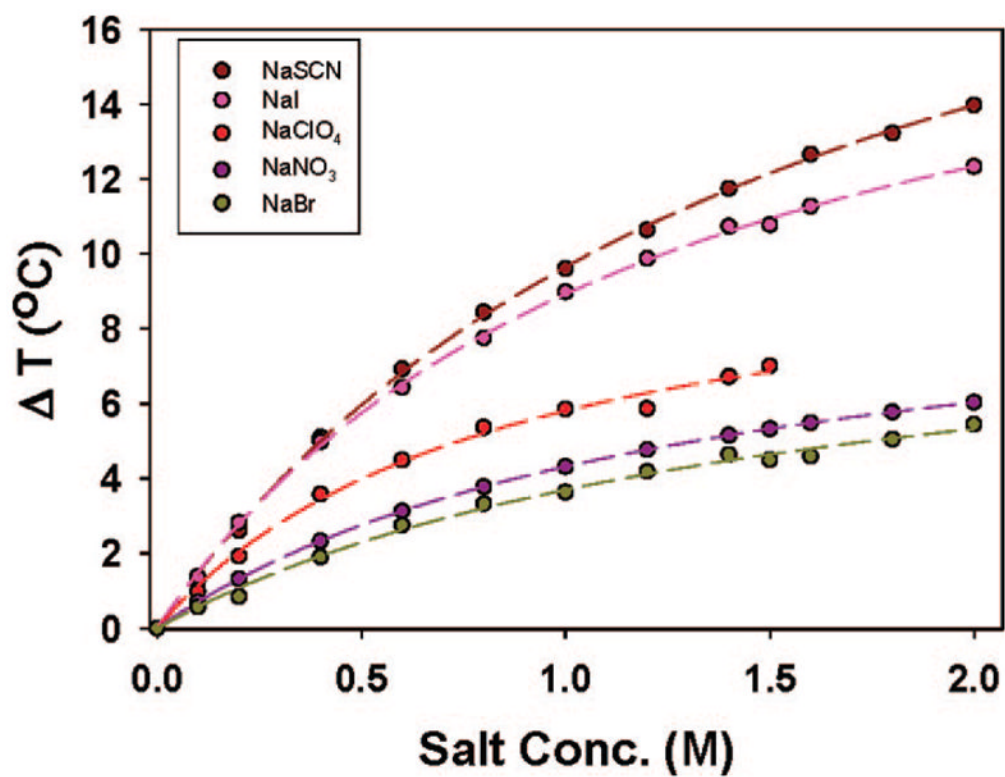


Figure 5. Residual LCST vs salt concentration data for the chaotropic anions with ELP V₅-120 after subtracting out the linear portion of the data. The dashed lines represent Langmuir isotherm fits to the data points.

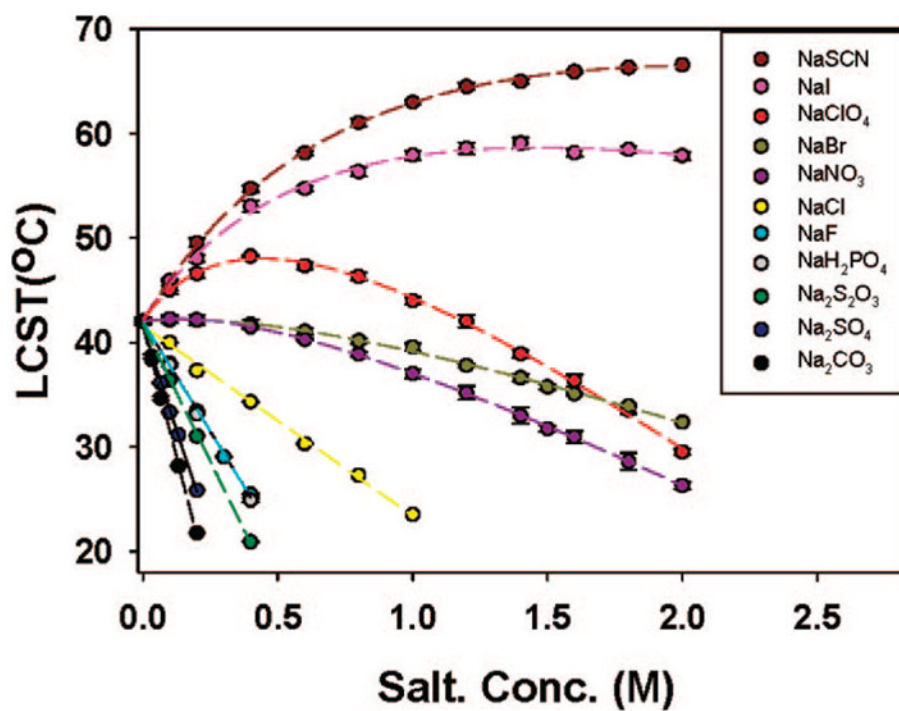


Figure 6. LCST vs salt concentration curves for ELP V₅A₂G₃-120 with a series of sodium salts. Each data point represents the average of eight measurements, and the standard deviations are within the size of the circles used to plot the data. The dashed lines are fits to the data using eqs 1 and 2.

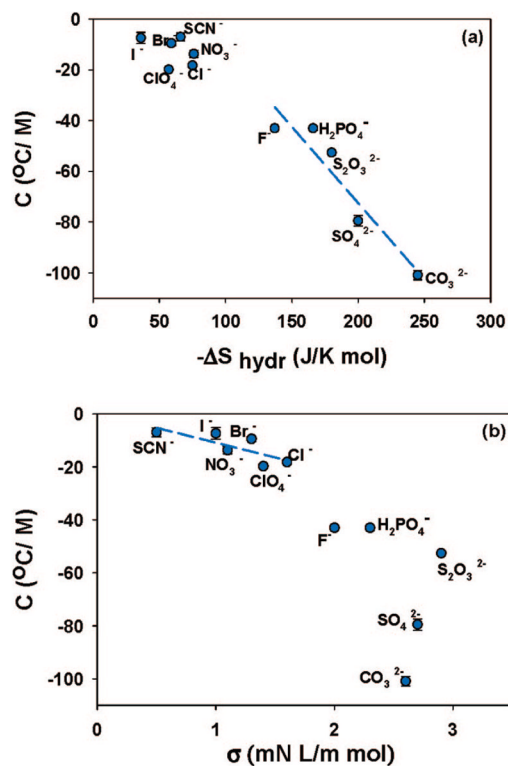


Figure 7. Plot of the linear slope, c , from eq 2 against (a) ΔS_{hydr} and (b) σ for ELP V₅A₂G₃-120 with 11 different sodium salts. The dashed blue lines are fits to the kosmotropes in (a) and the chaotropes in (b).

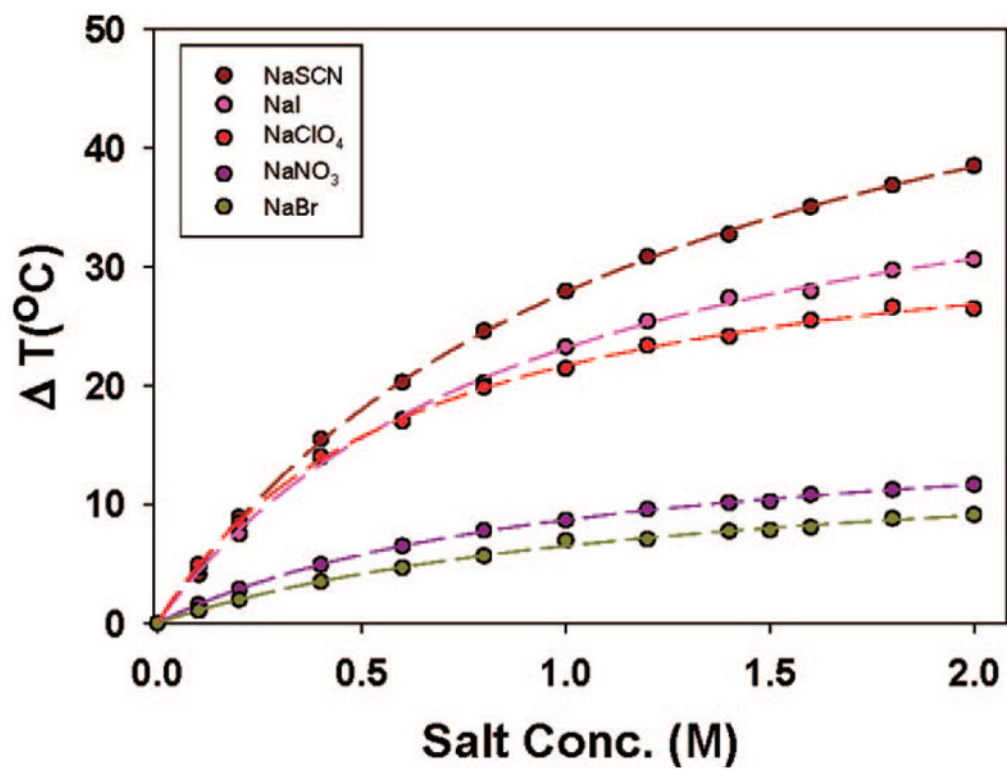


Figure 8. Residual LCST vs salt concentration data for the chaotropic anions with ELP V₅A₂G₃-120 after subtracting out the linear portion of the data. The dashed lines represent Langmuir isotherm fits to the data points.

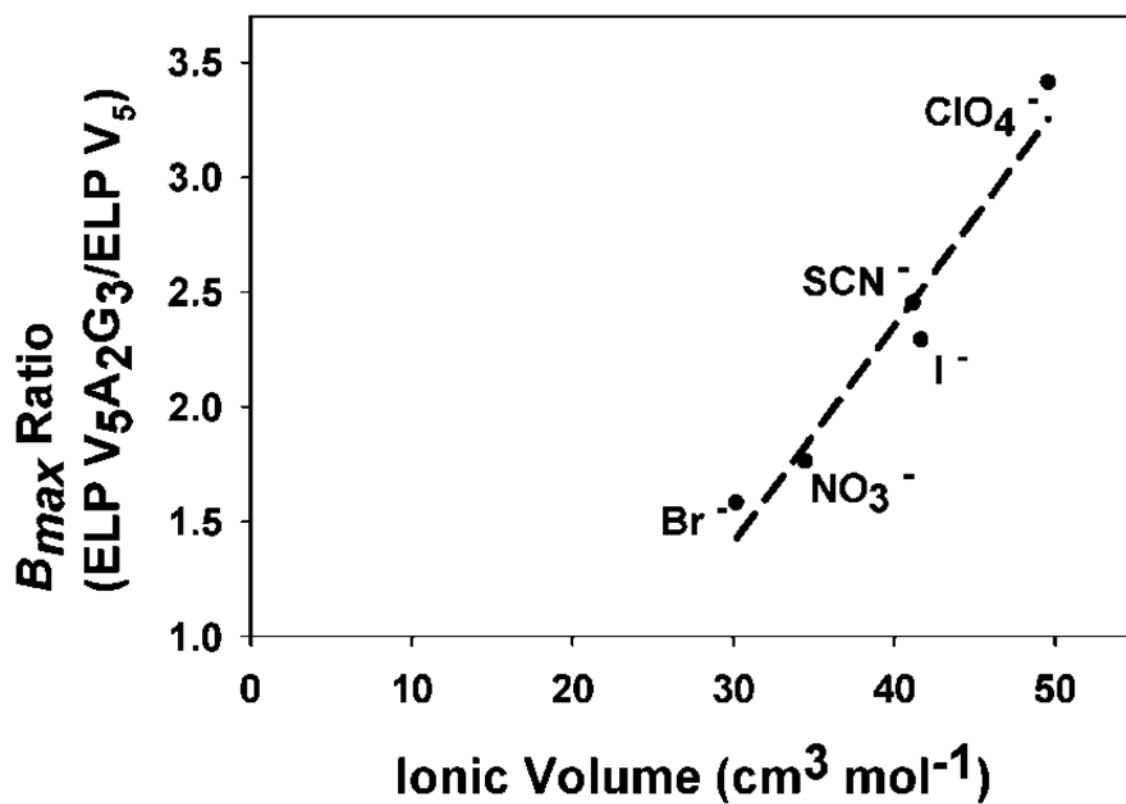


Figure 9.
Plot of the ratio of B_{\max} values for ELP V₅A₂G₃-120/ ELP V₅-120 vs ionic volume of chaotropes ions.

TABLE 1

Fitted Values from LCST Data of ELP V₅-120 and ELP V₅A₂G₃-120 with 11 Sodium Salts to Eqs 1 and 2^a

ion	ELP V ₅ -120			ELP V ₅ A ₂ G ₃ -120			ELPV ₅ A ₂ G ₃ -120/ELP V ₅ -120		
	<i>B</i> _{max}	<i>K</i> _A	<i>c</i>	<i>B</i> _{max}	<i>K</i> _A	<i>c</i>	<i>B</i> _{max} ratio	<i>K</i> _A	<i>c</i>
SCN ⁻	25.1	0.63	-6.6 ± 1.0	61.5	0.84	-7.0 ± 1.7	2.5		
I ⁻	19.9	0.81	-6.5 ± 0.7	45.7	1.0	-7.4 ± 2.2	2.3		
ClO ₄ ⁻	10.6	1.3	-12.5 ± 0.8	36.4	1.5	-20 ± 1.0	3.4		
Br ⁻	9.38	0.67	-7.3 ± 0.7	14.8	0.78	-9.4 ± 1.4	1.6		
NO ₃ ⁻	10.0	0.76	-8.8 ± 1.2	17.6	0.97	-14 ± 0.5	1.8		
Cl ⁻			-11.4 ± 0.4			-18 ± 0.5			
F ⁻			-26.3 ± 1.6			-43 ± 0.8			
H ₂ PO ₄ ⁻			-33.7 ± 1.8			-43 ± 1.0			
S ₂ O ₃ ²⁻			-54.4 ± 1.6			-53 ± 0.8			
SO ₄ ²⁻			-70.6 ± 2.4			-79 ± 2.1			
CO ₃ ²⁻			-77.0 ± 2.7			-100 ± 1.8			

^a *B*_{max} has about 10% error while the errors on the *K*_A values are smaller.